P3.36 An Evaluation of the Potential Impact of SAILS on the Warning Decision Making of the 31 May 2013 El Reno, OK Storm

Michael A. Magsig[1] and Marcus D. Austin[2]

[1]Warning Decision Training Branch, [2]OUN National Weather Service Forecast Office

1. INTRODUCTION

On May 19th, 20th, and 31st of 2013, a series of significant tornado outbreaks occurred in central Oklahoma (NCDC 2013; see also OUN WFO May 31-Jun 01, 2013 event webpage). As a result of the strong to violent tornadoes on May 19th and 20th, a high degree of public sensitivity to severe weather existed in the Oklahoma City metropolitan area on May 31st when the environment once again supported the threat of significant tornadoes in areas that had been devastated weeks before.

The environment on May 31, 2013 favored rapid evolution of supercell thunderstorms owing to Convective Available Potential Energy (CAPE) of over 5000 J/kg, 40-50 kts of 0-6km shear, 0-1km shear of 20-25 kts, supercell composites over 20, and significant tornado parameters around 3 (http://www.spc.noaa.gov/exper/ma_archive/). By late afternoon on Friday the 31st, the Storm Prediction Center issued a tornado watch highlighting a particular dangerous situation for intense tornadoes, very large hail, and damaging wind gusts. Given the day of the week, time of day, and the aftermath from the previous tornadoes within the threat area, there was a high degree of situation awareness within both the weather community and the public.

The May 31st event was unique for a number of reasons, including the widest tornado on record (4.18 km) near El Reno, OK (NCDC 2013), erratic tornado motions, multiple high-profile storm chaser injuries and fatalities, historic flash flooding, and a unique public response where widespread road gridlock resulted from a large number of people attempting to flee the tornado threat.

Corresponding Author: Mike Magsig
120 David L. Boren Blvd
Norman, OK 73072
Michael.A.Magsig@noaa.gov

The May 31st El Reno storm was well sampled by the experimental KCRI Weather Service Radar 88 Doppler (WSR-88D) and the operational KTLX WSR-88D which are located ~20 km apart. The rapid evolution of the El Reno storm coupled with the unusually large size and varying motion of the tornado close to two WSR-88Ds running different scan strategies affords a unique opportunity to evaluate recent volume scan strategy enhancements to the WSR-88D and its potential impact to warning decision making.

In the late spring of 2013 the NWS began implementing a new volume scan strategy called the Supplemental Adaptive Intra-Volume Low-Level Scan (SAILS; Crum et al. 2013). When using Volume Coverage Pattern 12 or 212 with SAILS enabled, the radar adds an extra 0.5 degree slice of reflectivity, velocity, and spectrum width data halfway through the normal volume scan. This effectively doubles the low-altitude temporal resolution of the data. On May 31st SAILS had not been implemented on the operational KTLX WSR-88D, so NWS forecasters did not have access to this data. The KCRI test WSR-88D collected SAILS data during this event, effectively increasing the low-altitude radar data temporal resolution from ~ 5 minutes to ~ 2.5 minutes.

One of the co-authors of this paper (Marcus Austin) was one of the warning forecasters for this event who used the KTLX WSR-88D data. Our analysis approach is to evaluate operational warning decision making from a KCRI SAILS perspective in light of the important warning decisions and communications that occurred during the event.

2. CONTINUOUS STREAM OF INFORMATION FOR THE MAY 31, 2013 EVENT

By augmenting standard warning products with Internet and social media communications, the OUN forecast office provided a more continuous stream of information during this high-impact event. In the 20 hours from 945 UTC on May 31 to 6 UTC on Jun 1, the OUN forecast office issued over 250 separate

communications. These included: the Hazardous Weather Outlook discussing severe weather potential for the day, event-specific Internet images (aka Graphicasts), a YouTube video briefing of anticipated event evolution, Twitter and Facebook posts for brief public messages and updates, NWSChat messages for NWS partners, a Public Information Statement for conveying tornado safety options, a Special Weather Statement providing a forecast for previous tornado recovery areas, a Significant Weather Advisory for providing information about developing storms when they are below severe criteria, as well as the Severe Thunderstorm Warning, Tornado Warning, and Flash Flood Warnings and warning updates in Severe Weather Statements and Flash Flood Statements. To review the communications for this event, see http://www.srh.noaa.gov/oun/?n=events-20130531-chronology. In reviewing the KCRI data and the communications during the event, the main benefit of the extra 0.5 degree SAILS tilts related primarily to warnings, follow-up statements, and Twitter/Facebook posts for reasons discussed in the following sections.

3. IMPROVEMENTS WITH SAILS

Doubling the temporal resolution of low-altitude radar data noticeably enhances the human pattern matching and feature detection. Features move and evolve in a more continuous fashion, and increased sampling leads to better resolving peak values and increased forecaster confidence in storm evolution. In this event the SAILS had more of an impact on warning decision making after the storm matured when features in low levels were more critical to the warning decision.

The El Reno storm initiated around 2115 UTC, and the storm quickly developed middle and upper-level radar signatures associated with severe hail and wind, including increases in storm-top divergence and reflectivities above the freezing level. Because the initial critical cues in the radar data came from radar tilts above the 0.5 degree tilt, the extra SAILS tilt had a limited impact on the decision making early in the storm's life, except to provide confidence that the hail core aloft had not reached the ground and the severe weather threat was not as imminent.

The first significant improvement with SAILS data occurred when the initial hail core descended to the 0.5 degree level at 2151 UTC (Fig 1). Even with 2.5 minute resolution data, SAILS showed significant changes in reflectivity values in the hail core, suggesting higher resolution data may be required to fully resolve intensity changes in relatively large hail cores. SAILS also better resolved the weakening of the first significant hail core pulse after 2201 UTC and the subsequent development of a second hail core pulse at 2216 UTC. While the storm had yet to develop significant supercell structures in low-levels, there was a brief small-scale area of weak gate-to-gate rotation that developed and quickly weakened from 2211-2216 UTC. The evolution of this feature was very hard to resolve without the extra SAILS tilt.

The second significant improvement with SAILS data occurred when the storm matured and started forming supercell structures (strong inflow and rear-flank downdraft (RFD) surges) at the 0.5 degree level around 2227 UTC (Fig 2). As a storm merger began, the SAILS data better resolved the initial RFD surge with the northern storm, which was a critical cue for issuing a tornado warning. The extra SAILS tilts at 2232 UTC and 2242 UTC showed some of the stronger rotation observed and provided a much more continuous picture of cyclic mesocyclogenesis from 2247-2252 UTC. The SAILS data also resolved the rapid evolution of a unique extremely sharp left-flank hail curtain at 2247 UTC.

The third significant improvement with SAILS data occurred with the development of the El Reno tornado (Fig 3). The extra SAILS tilt detected the strong localized rotation with tornado formation at 2303 UTC and provided 2.5 minutes of earlier detection than the traditional volume scan strategy. The tornado motion to the E-SE, E, and then N-NE was clearly resolved and resolved sooner with the extra SAILS tilts. The SAILS data also provided key snapshots of the massive RFD intensification and position of the tornado threat.

The fourth significant improvement with SAILS data occurred with the development of an anticyclonic tornado and subsequent second large RFD surge (Fig 4). The extra SAILS tilt first detected the significant tornado vortex signature of an anticyclonic tornado at 2329 UTC. It also more clearly captured the E-SE

and then S movement of the anticyclonic vortex. The extra SAILS tilt also resolved a tornado reflectivity eye with the El Reno tornado in its later stages, as is commonly observed in mobile high-resolution radar datasets (Wurman et al. 2013). As another large RFD surge developed, the SAILS data clearly resolved the development of another left-flank sharp hail curtain, which rotated 45 degrees into a similar configuration as observed earlier (see 2308 Fig 3 and 2351 Fig 4).

The strong inflow, RFD velocities, and rotation are significant supercell structures that are critical cues in warning decision making. Fig 5 shows that SAILS provided a more continuous perspective on longer term trends like the max inflow velocity increase from 2220-2315 UTC. Fig 5 also shows SAILS provided critical consistent trend information on RFD maximum velocities and maximum rotational velocity trends for the El Reno storm's mesocyclone and tornado vortex signatures. This storm contained numerous notable features that had time scales ranging from 5 minutes to 55 minutes (Fig 6). With the ~2.5 min increase in temporal resolution of SAILS low-altitude radar data, the evaluation of important features with this storm is significantly improved. Even with the longer-duration intensification processes like the 55 minute increase in inflow, SAILS increased confidence faster of an intensifying storm with the persistent increase in inflow strength observed.

4.1 UNIQUE STORM FEATURES – SHARP LEFT-FLANK HAIL CURTAIN

The sharp left-flank hail curtain began to form during the merger of two storms (Fig 7). Initially at 2229 UTC there were two deep reflectivity cores with separate storms, but as the northern storm's RFD continued to surge, a high-reflectivity core developed aloft at 2235 UTC along the leading edge of the RFD gust front at the location that the cores aloft were merging. By 2240 UTC, a second core aloft rapidly began to grow in size on the eastern half of the mid-level mesocyclone. This second core is the primary origin of the sharp left-flank hail curtain that evolves rapidly in the next five minutes.

Between 2240 and 2245 UTC, a radical change in orientation of the echo aloft began (Fig 8). The high reflectivities in the core quickly became elongated into a sharp curtain aloft, which sharpened up at 0.5 degrees five minutes later at 2250 UTC. While the hail curtain high reflectivities were initially located within the mesocyclone, they quickly transitioned to outside the peak velocities of the mesocyclone and became co-located with a strong mid-level convergence signature (see 3.1 degrees at 2306 UTC in Fig 8). As the mesocyclone and RFD intensified, the hail curtain rotated 45 degrees and ultimately was drawn into the back side of the hook echo.

4.2 UNIQUE STORM FEATURES – EL RENO MESOCYCLONE

The El Reno tornado vortex signature developed from a relatively weak and small RFD initially (Fig 9). The tornado vortex signature developed as a smaller velocity couplet within a very broad mesocyclone aloft (3-4km AGL) and immediately started moving to the east-southeast. As the RFD associated with the tornado vortex signature rapidly intensified and grew to the spatial scale of the storm's deep inflow velocity peak, an extremely intense and more symmetric mesocyclone developed to the left of the tornado's initial track (see 2.4 degrees 2301-2317 UTC in Fig 10). As the mid-level mesocyclone matured, the tornado vortex signature moved progressively left of the initial track. The evolution of the rotation signatures suggests the motion changes of the tornado may have been associated with a somewhat unusual mesocyclone evolution. Our experience has been that many times the symmetric organized mid-level mesocyclones precede tornadogenesis rather than growing larger and more symmetric following tornadogenesis.

Wurman et al. (2013) showed that three of the storm researcher fatalities in this event were killed by an erratic fast moving sub vortex from what they call a violent tornado/multiple-vortex mesocyclone. Our observations of the mesocyclone evolution are consistent with the possibility that the unusual size and motion of the tornado was associated with a unique feedback between a large tornado with an expanding large RFD and intensifying larger-scale mesocyclone.

4.3 UNIQUE STORM FEATURES - SEEDING

The rear-flank of the El Reno storm was seeded by multiple storms throughout its lifetime. The first

storm merger (Fig 2) resulted in a precipitation-laden mesocyclone core that remained broad for some time and was only weakly tornadic. Once the merger was complete, and the storm became more isolated, the large long-track El Reno tornado formed.

Just before the El Reno tornado formed, a new cell started to intensify on the trailing cold pool of the El Reno storm (see Fig 10). The 0.5 degree data showed three fine lines on radar: the rear-flank cold pool of the El Reno storm, the dryline, and a southward moving boundary believed to be the front. The cell that developed on the El Reno storm's cold pool near the dryline intensified rapidly, and seeded the El Reno storm throughout its lifetime. The post-El Reno seeded mesocyclones remained broad in low levels (see 2356 UTC in Fig 4), like during the initial seeding from the first storm merger, and the tornadoes were not as large or damaging as El Reno. This east-west configuration resulted in training supercells with very heavy rain and historic flash flooding in the Oklahoma City metro.

5. DISCUSSION

Doubling the temporal resolution of low-altitude reflectivity, velocity, and spectrum width data at 0.5 degrees from ~5 min to ~2.5 min with SAILS noticeably enhanced the radar analysis for warning decision making in this event. Specifically, the extra SAILS tilt provided 2.5 min earlier detection of: low-level mesocyclogenesis preceding the initial tornado, the El Reno tornado, an anticyclonic tornado, hail core intensity changes, intensity changes in inflow/RFD/rotation, and mesocyclone/tornado motion changes. In addition to earlier detection, the more continuous depiction of radar signatures provided for more confidence in trends required for warning decisions.

Given that SAILS only provides extra low-altitude sampling, there are situations in which SAILS does not significantly change warning decision making. Early in the El Reno storm's evolution when the critical cues for severe thunderstorm warning are in upper levels, SAILS had less of an impact, except to confirm that the developing hail core aloft had not yet reached low levels. Even when radar signatures are aloft, SAILS can provide for better motion estimates and for more accurately associating spotter hail reports with hail cores. With storms at longer distances where sampling reaches middle levels, SAILS may provide more useful information for severe hail warning decisions.

As storms develop more mature low-level structure, SAILS becomes essential in communicating key intensity and location information commonly conveyed in the continuous stream of information of warnings, follow up statements, and social media interaction such as Twitter, Facebook, and NWSchat.

There are a few limitations with the first version of SAILS. Not having Dual-Pol variables produces offsets in times between multiple product overlays, and it prevents enhanced hail detection and tornado debris detection. Build 16 of the Radar Product Generator, anticipated to be fielded in 2015, will address this important need (Mike Istok NPI Lead personal communication).

The SAILS labeling and navigation controls in AWIPS could also be improved. AWIPS treats the extra SAILS tilt as a single-tilt volume scan, which affects time matching and navigation controls in unique ways for four panels and all tilts. With future improvements to SAILS to potentially provide 1 minute scans with Meso-SAILS (Mike Istok NPI Lead personal communication), more attention needs to be paid on how to manage the data. Larger frame counts are going to be required to view the same duration, and the forecaster may require more control over time matching.

There are a number of aspects of the El Reno event that raise further questions to explore. What was unique about the El Reno storm such that it produced the widest tornado on record? In our analysis, there were some unique features observed with the El Reno tornado. A storm merger immediately preceded the tornadogenesis, as has been previously observed with some significant tornadoes (Burgess and Magsig 1993, Lee et al. 2006, Tanamachi et al. 2014). This merger was unique in the resulting unusually sharp and rapidly developing left-flank hail curtain that rotated 45 degrees and was eventually drawn into the back side of the hook echo nearby the very large and damaging RFD. Such a pronounced sharp gradient in hydrometeors has the potential to impact cold pool

dynamics and may be worth investigating what affect, if any, the hail curtain had on the genesis of the El Reno tornado. A subsequent new RFD surge and less sharp left-flank hail curtain evolution occurred after the El Reno tornado without a storm merger that looked very similar to the first only the mesocyclone rotation remained broad as it was strongly seeded by a storm that initiated on the El Reno storm's cold pool.

Another intriguing observation with the El Reno tornado vortex signature was that there was an unusual RFD and mid-level mesocyclone evolution that appears to be correlated with the unusual motion changes of the tornado. The tornado initially developed along the small modest RFD within a broad mesocyclone aloft, but further intensification and growth of the RFD to the spatial scale of the storm's deep inflow resulted in an extremely strong, large, and more symmetric mid-level mesocyclone after tornadogenesis. The complex development of the larger mesocyclone interacting with the tornado along the expanding and intensifying RFD could be related to the larger-scale changes in tornado motion and this record observation of tornado width.

Another question for researchers and storm modelers to explore is what role did seeding play in limiting the tornado production on this day? The El Reno tornado was unique among all storms this day in tornado characteristics. Many of the other circulations had seeding issues in the mesocyclones from other storms that may have been destructive. Had the El Reno storm continued producing extremely large and damaging tornadoes as it moved into the unusually gridlocked traffic from masses of people fleeing the tornado in the Oklahoma City metro, the number of auto fatalities could have been unprecedented. Was an even greater disaster avoided due to a storm initiating on the cold pool of the El Reno storm? How predictable was this and the historic flash flooding following the El Reno tornado?

6. ACKNOWLEDGEMENTS

The authors would like to thank Steve Kruckenberg from the Norman Forecast Office for assembling the products timeline used in this analysis. We would also like to thank Alexander Zwink from WDTB for assistance in generating SAILS radar data from the KCRI WSR-88D.

7. REFERENCES

Crum, T., S. D. Smith, J. N. Chrisman, R. E. Saffle, R. W. Hall, and R. J. Vogt, WSR-88D radar projects – update 2013. Extended Abstract, 29th Conf. on Environmental Information Processing Technologies, Austin, TX, Amer. Meteor. Soc., 8.1

Burgess D.W. and M. A. Magsig, 1993: Radar evolution of the Red Rock, Oklahoma supercell of April 26, 1991. Preprints, *17th Conf. on Severe. Local Storms*, St. Louis, MO, Amer. Meteor. Soc., 97-108.

Lee B. D., B. F. Jewett, and R. B. Wilhelmson, 2006: The 19 April 1996 Illinois Tornado Outbreak. Part II: Cell Mergers and Associated Tornado Incidence. *Wea. Forecasting*, **21**, 449–464.

NCDC, 1998: Storm Data. Vol. 55, Nos. 466-467, 684 pp.

Tanamachi, R. L., P. L. Heinselman, L. J. Wicker: 2014 Investigation of a cell merger accompanying cyclic tornado production. Preprints, *27th Conf. on Severe. Local Storms*, Madison, WI, Amer. Meteor. Soc.

Wurman J., K. Kosiba, 2013: Finescale Radar Observations of Tornado and Mesocyclone Structures. *Wea. Forecasting*, **28**, 1157–1174.

Wurman J., K. Kosiba, P. Robinson, and T. Marshall, 2014: The Role of Multiple-Vortex Tornado Structure in Causing Storm Researcher Fatalities. *Bull. Amer. Meteor. Soc.*, **95**, 31–45.

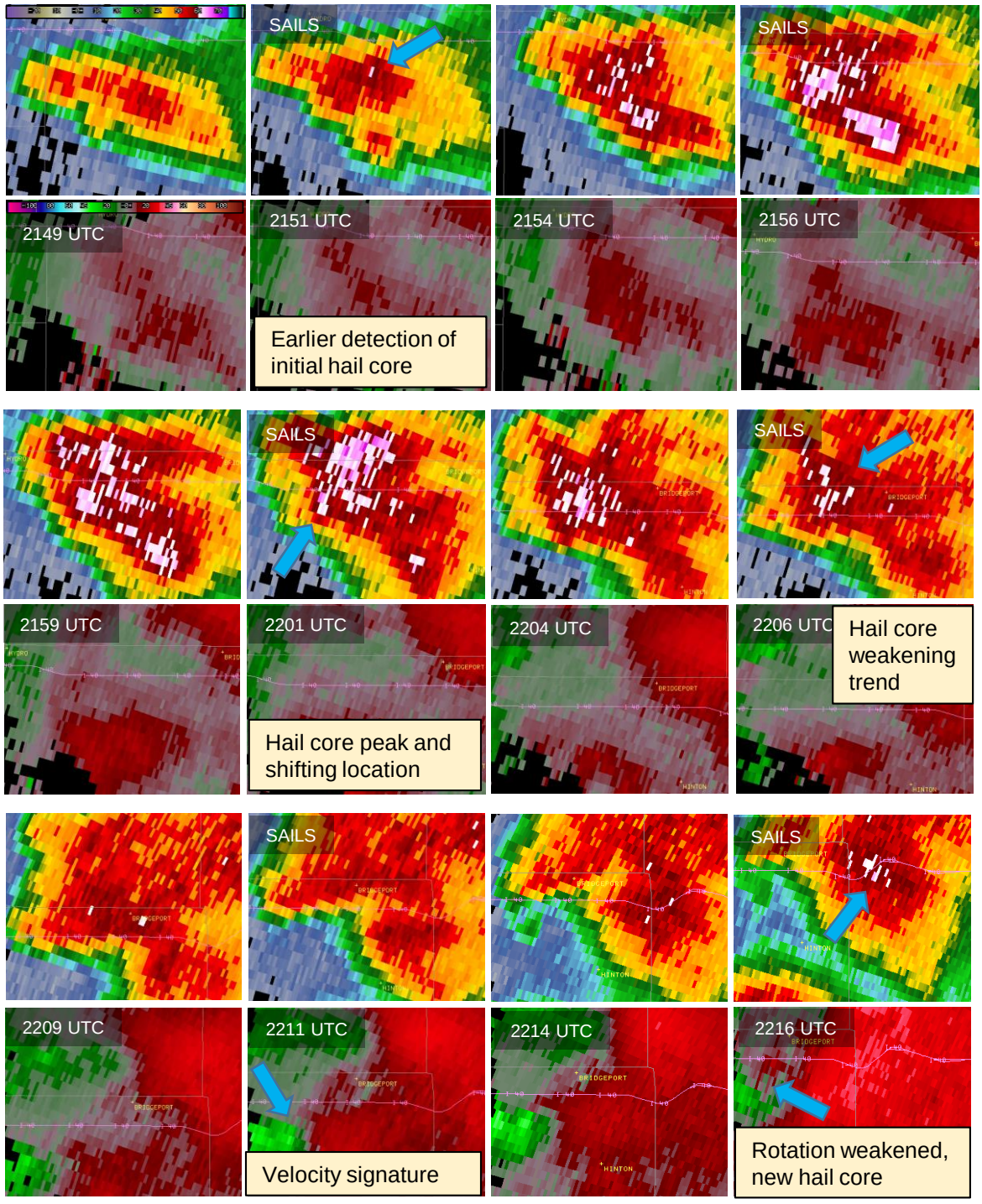

Fig 1. 0.5 degree reflectivity (top) and base velocity (bottom) sequence from 2149-2216 UTC from KCRI showing hail core pulse life cycle and weak rotation. Extra SAILS tilt detected intensity changes of hail core and rotational signature sooner.

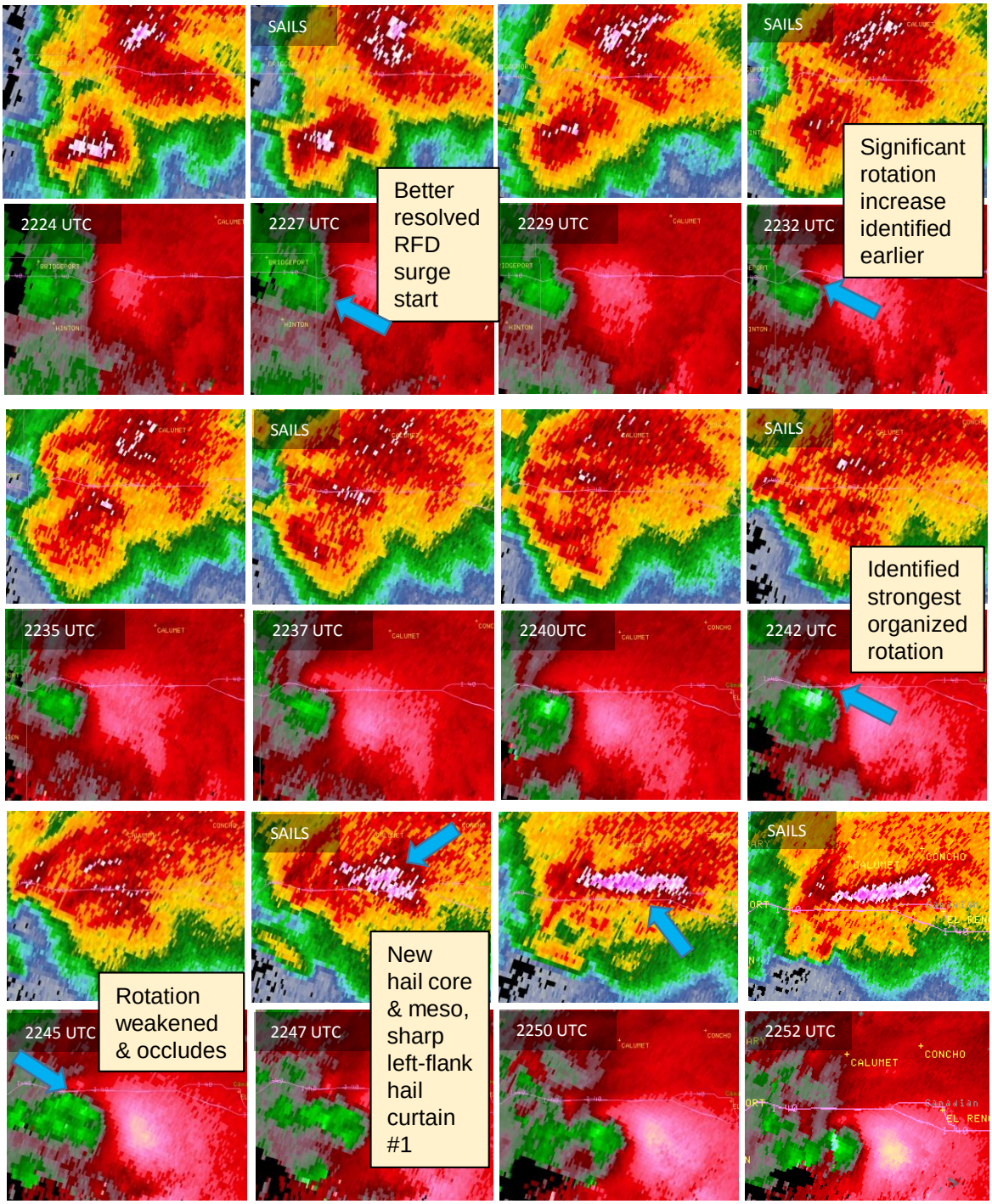

Fig 2. Same as in Fig 1 but for 2224-2252 UTC. Extra SAILS tilt detected first significant RFD surge of this storm as a cell to the south merged into the strong low-level convergence of the updraft. The extra SAILS tilt resolved the stronger times of rotation, and it better depicted the cyclic mesocyclone occlusion process and the formation of a sharp left-flank hail curtain.

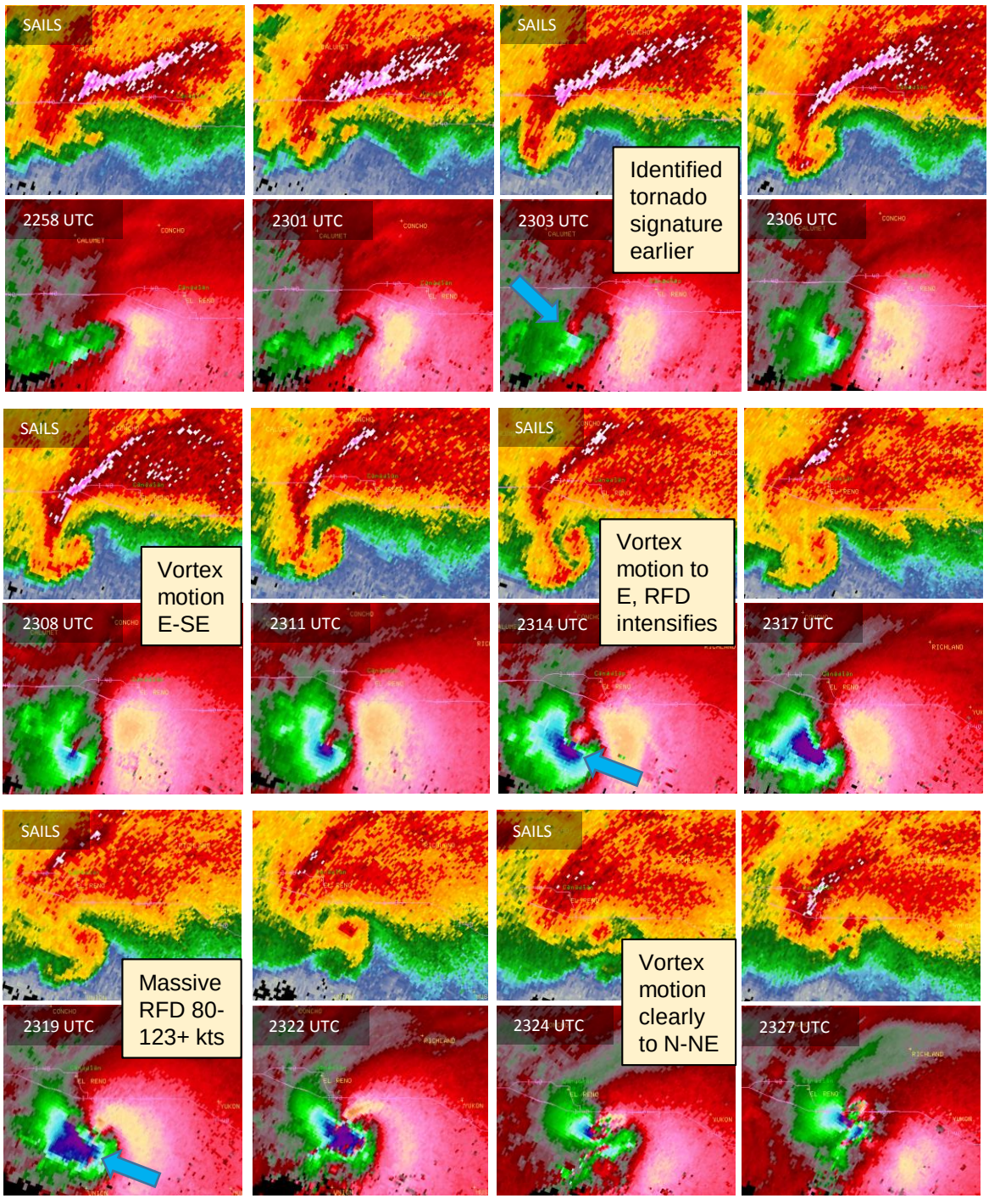

Fig 3. Same as in Fig 1 but for 2258-2327 UTC and showing tornadogenesis and massive RFD intensification. Extra SAILS tilt detected El Reno tornado sooner and clearly depicted vortex motions E-SE, E, and then N-NE.

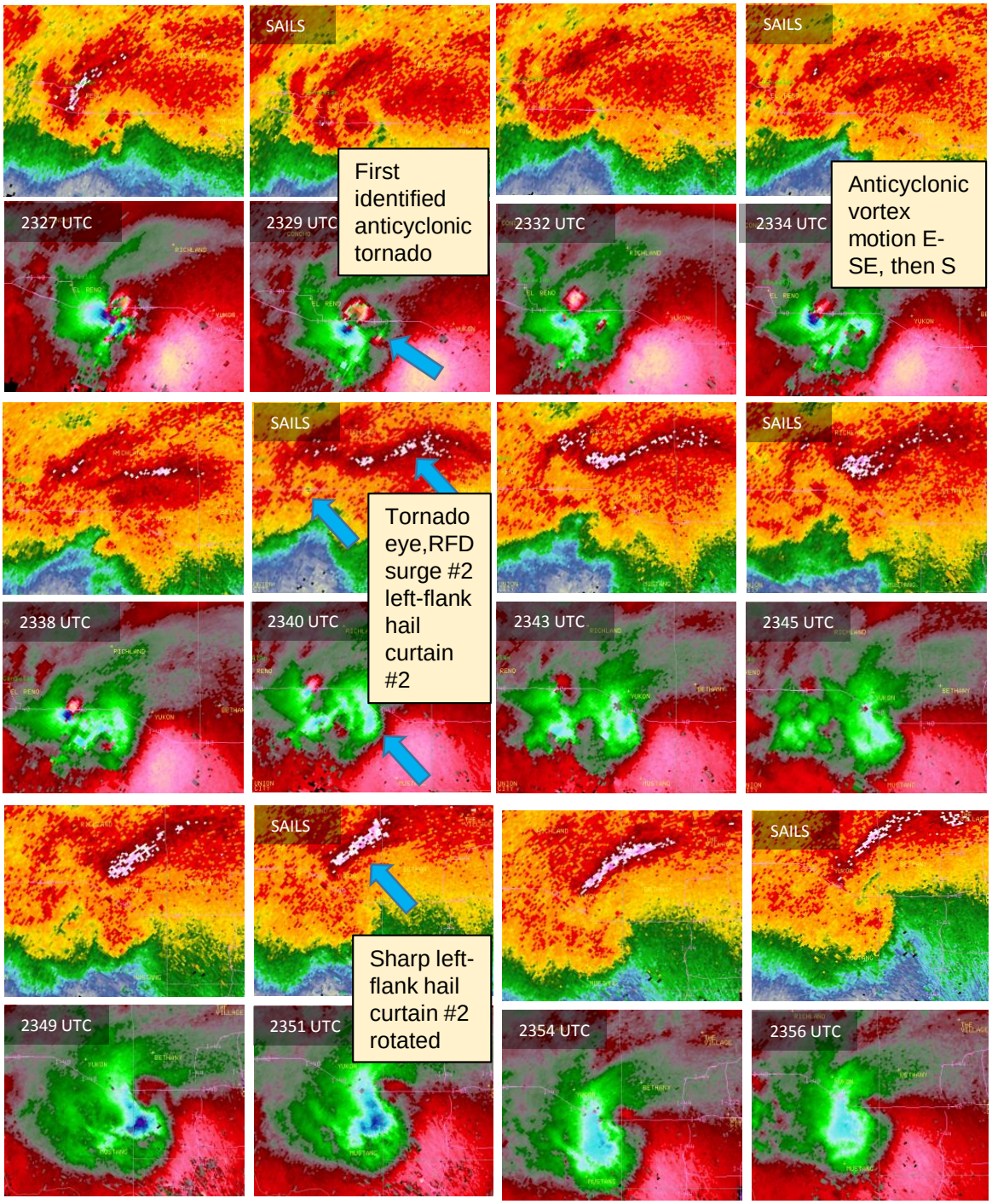

Fig 4. Same as Fig 1 but for 2327-2356 UTC. Extra SAILS tilt first detected anticyclonic tornado and better tracked motion E-SE then S. SAILS also detected El Reno tornado eye and better resolved El Reno demise, RFD surge #2, and rotation of left-flank hail curtain #2.

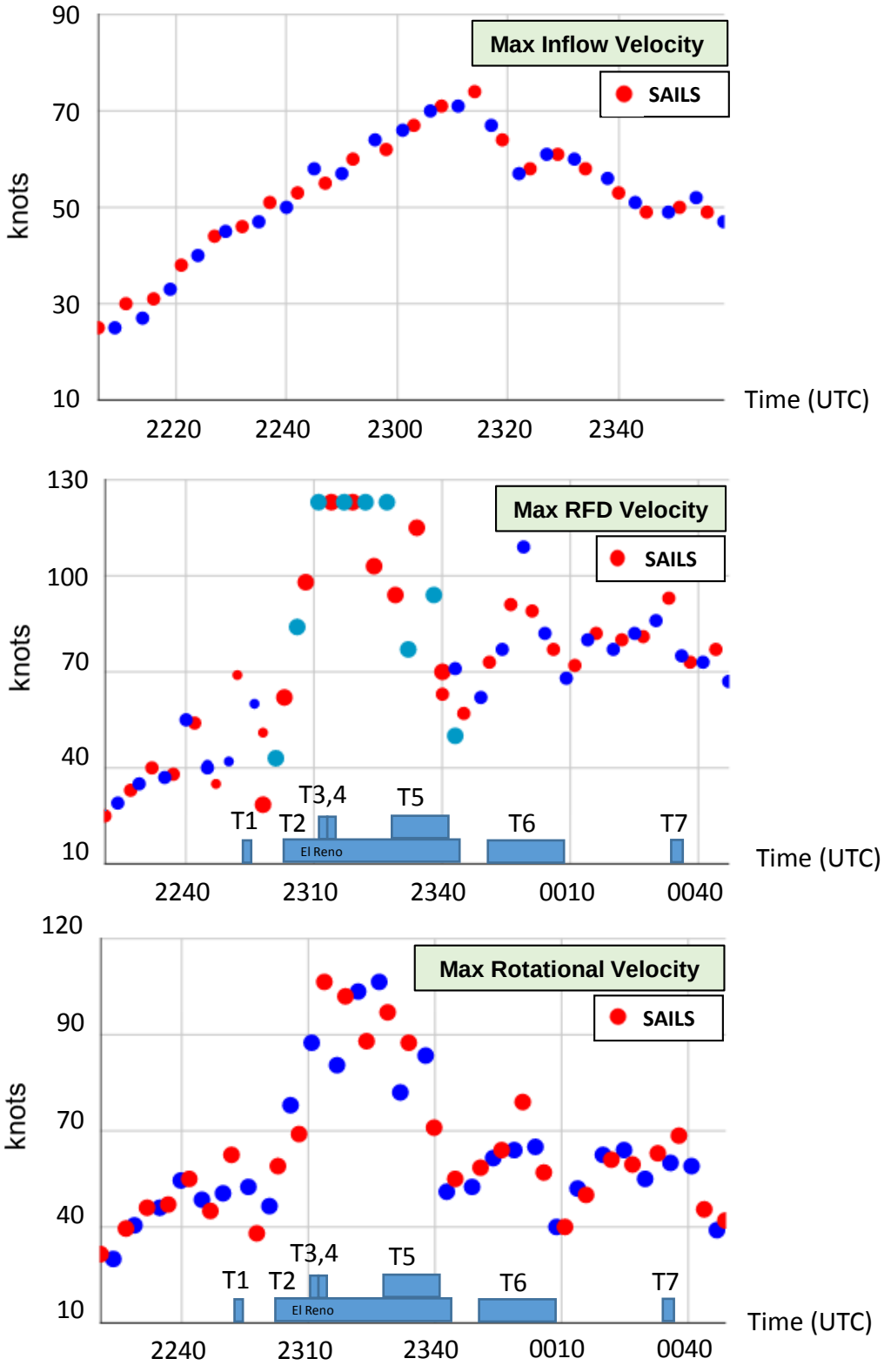

Fig 5. KCRI 0.5 degree maximum radial inflow velocity (top), maximum RFD base velocity (middle), and maximum rotational velocity (bottom). Red dots are extra SAILS tilt. Tornadoes 1-7 annotated on middle and bottom.

Notable Features	Time (UTC)	Duration (min)
1st Hail Core Intensifies	2146-2201	15
1st Hail Core Weakens	2201-2211	10
S Cell Hail Core Intensifies	2214-2221	7
N Cell Hail Core Intensifies	2211-2221	10
Inflow Increase	2219-2314	55
RFD1 Surge (Meso 1)	2224-2242	18
Sharp Left-Flank Hail Curtain1	2242-2250	8
Rotation of Sharp Left-Flank Hail Curtain1	2250-2308	18
RFD2 Surge (Meso 2)	2245-2256	11
Balanced Tornado Vortex	2301-2306	5
RFD3 Surge Massive (Meso 3)	2303-2319	16
Tornado North Jog	2319-2329	10
Sharp Left-Flank Hail Curtain2	2334-2443	9
Tornado Weakens	2338-2349	11
Rotation of Sharp Left-Flank Hail Curtain2	2340-2354	14
Anticyclonic Tornado	2322-2329	7
Anticyclonic Tornado South Jog	2332-2340	8
RFD4 Surge Large (Meso 4)	2332-2359	27

Fig 6. Duration of notable features for the El Reno storm. The 2.5 min temporal resolution with the extra SAILS tilt resolved many of these features much better.

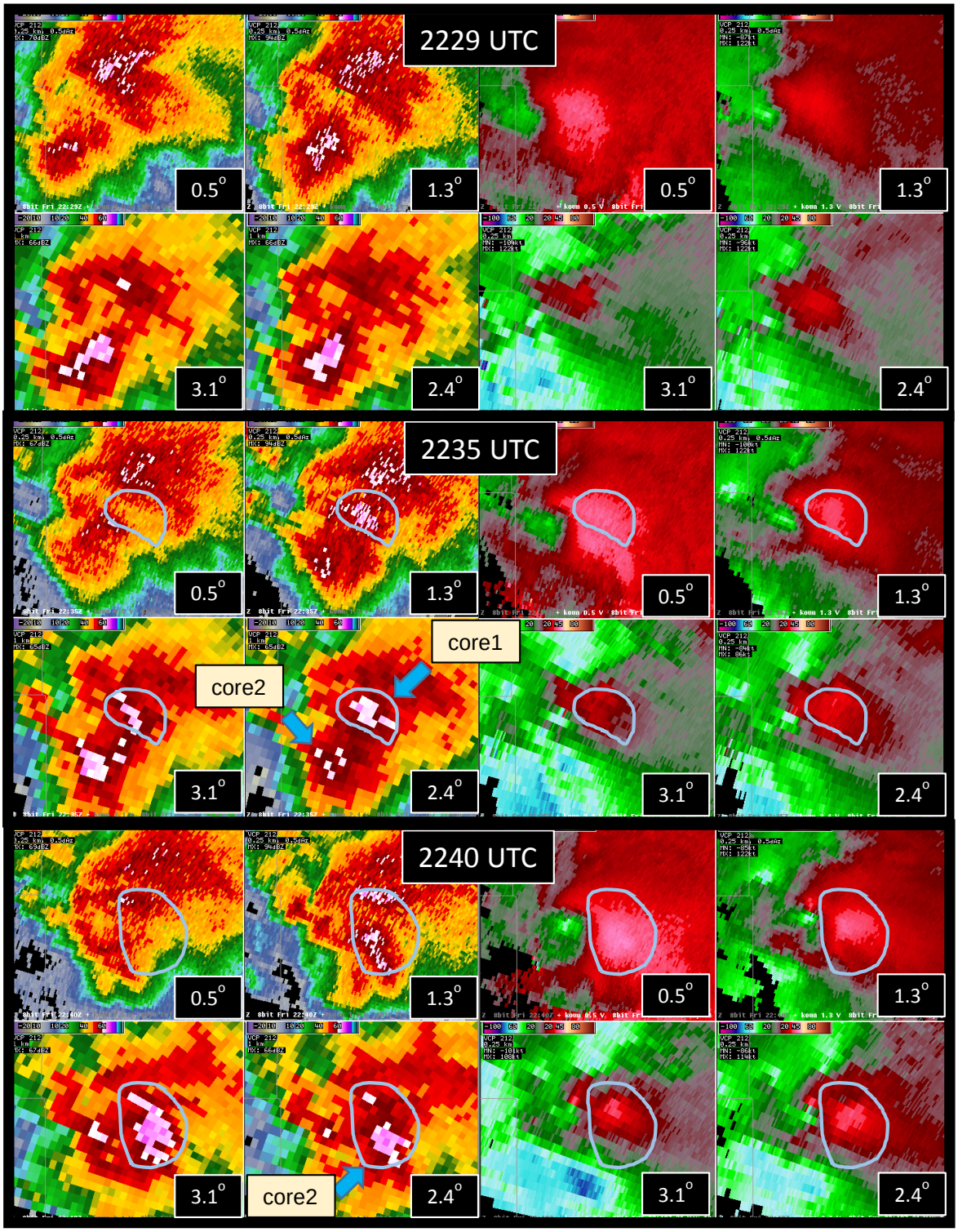

Fig 7. Four panel reflectivity (left) and base velocity (right) with 0.5, 1.3, 2.4, and 3.1 degrees at 2229 UTC (top), 2235 UTC (middle), and 2240 UTC (bottom) from KCRI showing storm merger. Following a surge in RFD, two mid-level reflectivity cores rapidly developed at the intersection of their precipitation echoes. Core 2, which formed inside the organizing mid-level mesocyclone, is the origins of the sharp left-flank hail curtain. Grey overlay indicates the location of the core aloft.

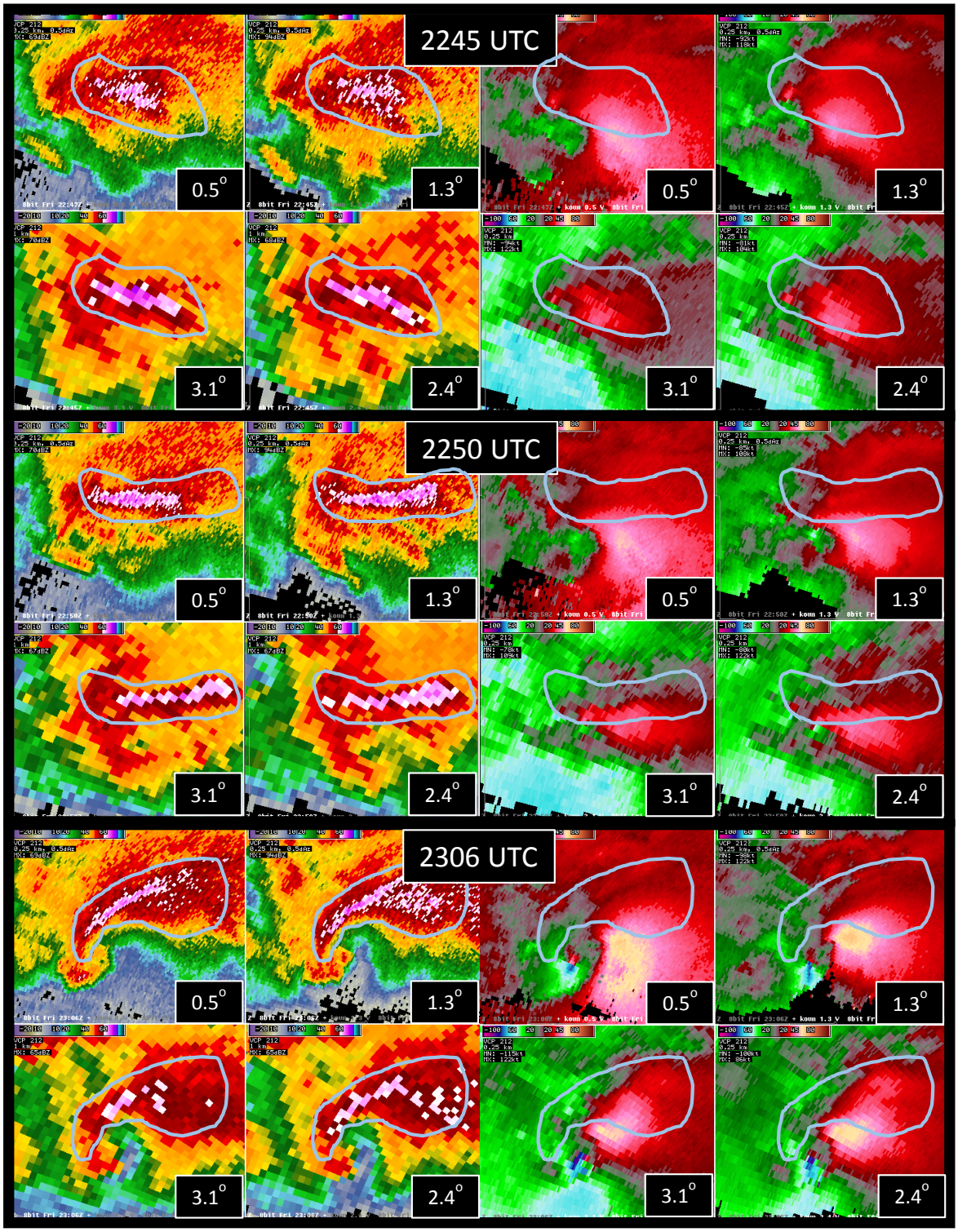

Fig 8. Same as Fig 8 but for 2245 UTC (top), 2250 UTC (middle), and 2306 UTC (bottom) showing the rapid formation of the sharp left-flank hail curtain. As the curtain descended, it began to shift outside the mesocyclone, eventually becoming co-located with strong mid-level convergence.

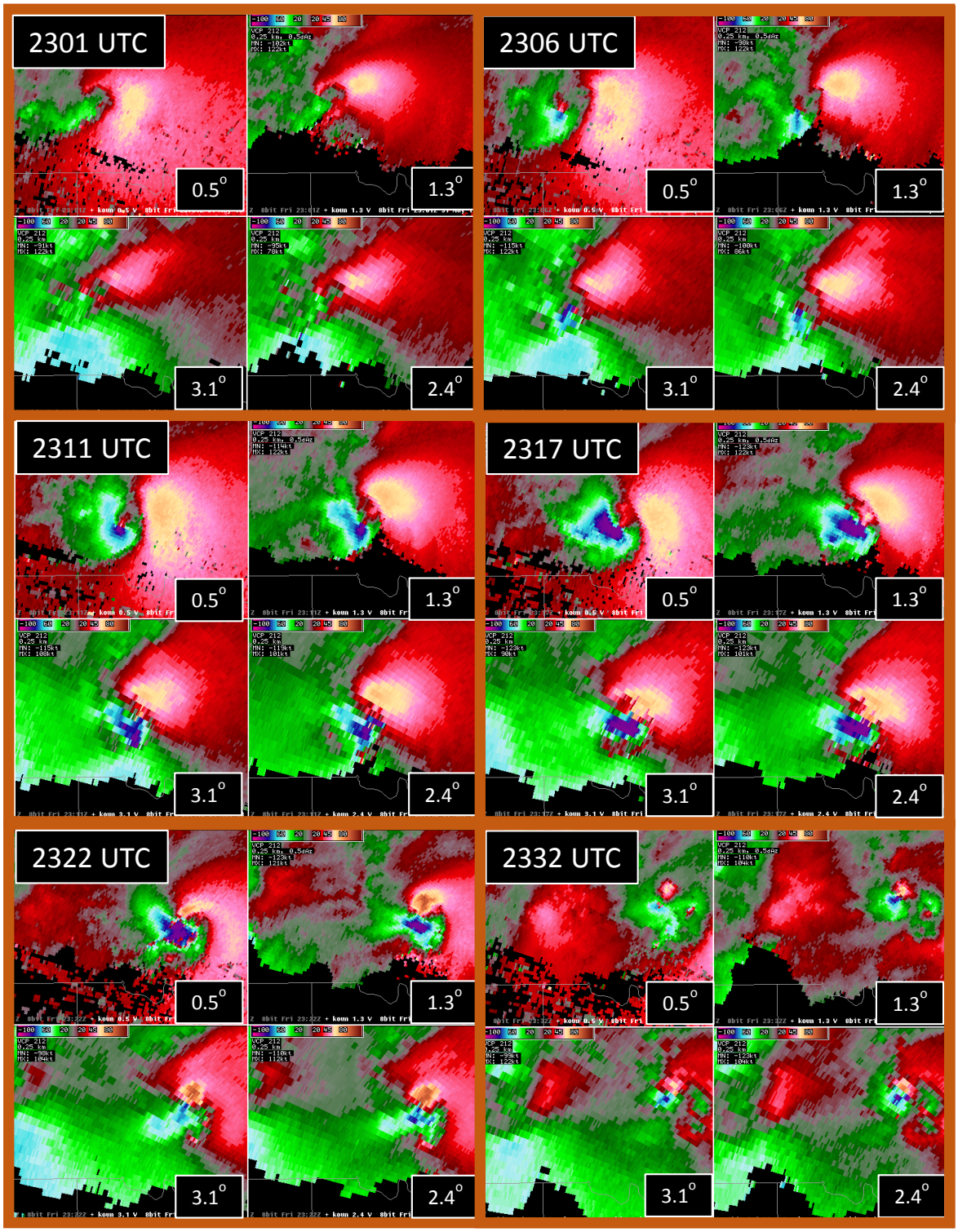

Fig 9. Four panel base velocity for 2301-2332 UTC showing an initial weak RFD which grew and intensified significantly after tornadogenesis, eventually forming an intense symmetric mesocyclone aloft (see 2.4 degrees from 2301-2317 UTC).

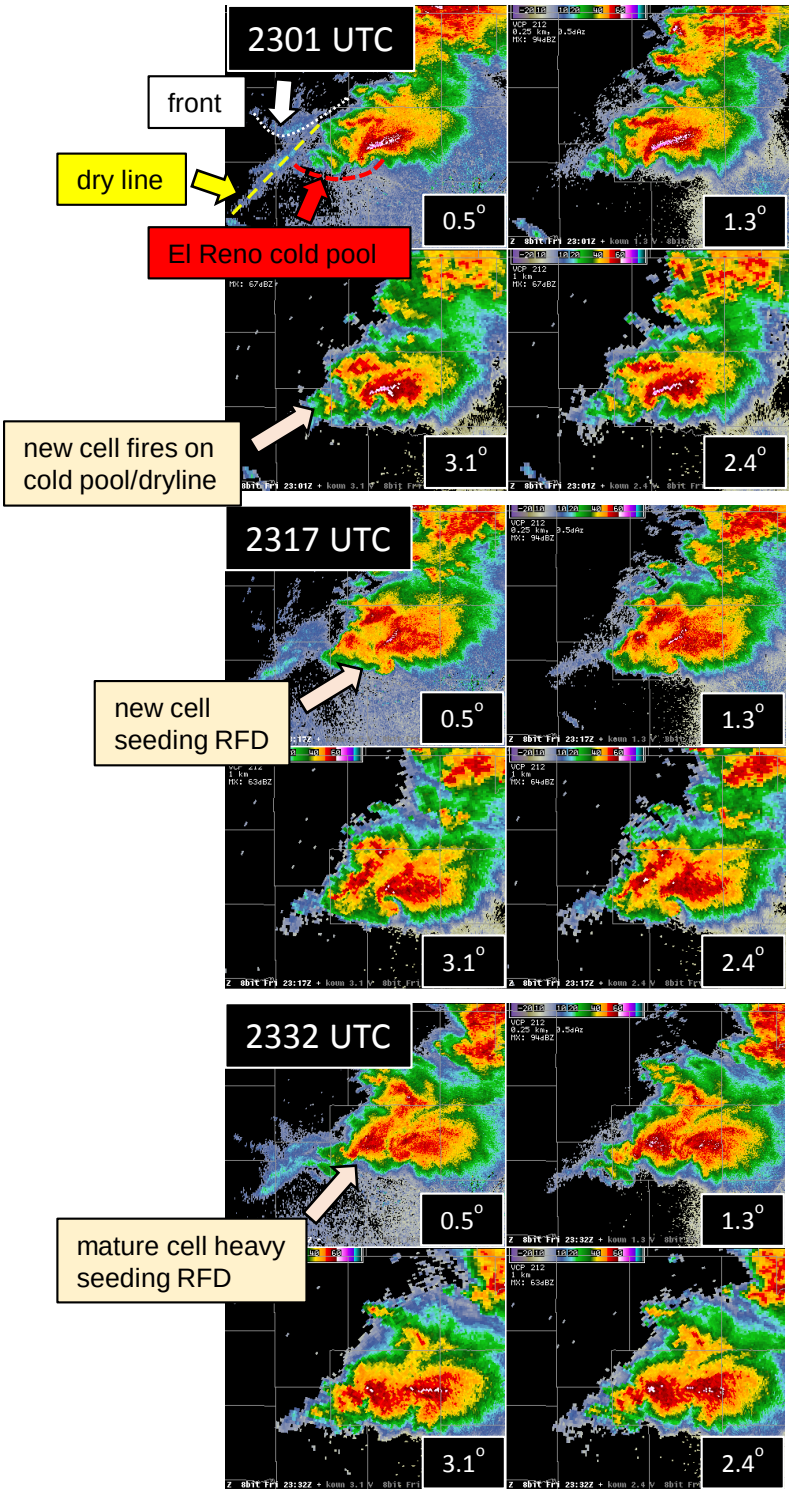

Fig 10. Four panel reflectivity with 0.5, 1.3, 2.4, and 3.1 degrees at 2301 UTC (top), 2317 UTC (middle), and 2332 UTC (bottom) from KCRI showing a new cell seeding RFD of El Reno storm. Fine lines at 0.5 degrees (top left) indicate the seeding cell formed on the El Reno storm's trailing cold pool near the dryline. The trailing storm significantly seeded the El Reno Storm.